

See discussions, stats, and author profiles for this publication at: <https://www.researchgate.net/publication/38076711>

Quantitative Phosphoproteomic Analysis of the STAT3/IL-6/HIF1 alpha Signaling Network: An Initial Study in GSC11 Glioblastoma Stem Cells

ARTICLE *in* JOURNAL OF PROTEOME RESEARCH · NOVEMBER 2009

Impact Factor: 4.25 · DOI: 10.1021/pr9007927 · Source: PubMed

CITATIONS

64

READS

129

20 AUTHORS, INCLUDING:



[Arugadoss Devakumar](#)

Indiana University Bloomington

5 PUBLICATIONS 185 CITATIONS

[SEE PROFILE](#)



[Stone Shi](#)

Amgen

23 PUBLICATIONS 1,419 CITATIONS

[SEE PROFILE](#)



[Yongjie Ji](#)

University of Texas MD Anderson Cancer C...

12 PUBLICATIONS 507 CITATIONS

[SEE PROFILE](#)



[Frederick F Lang](#)

University of Texas MD Anderson Cancer C...

211 PUBLICATIONS 9,343 CITATIONS

[SEE PROFILE](#)

Quantitative Phosphoproteomic Analysis of the STAT3/IL-6/HIF1 α Signaling Network: An Initial Study in GSC11 Glioblastoma Stem Cells

Carol L. Nilsson,^{*†} Roslyn Dillon,[†] Arugadoss Devakumar,[†] Stone D.-H. Shi,[†] Michael Greig,[†] John C. Rogers,[‡] Bryan Krastins,[§] Michael Rosenblatt,[‡] Gregory Kilmer,[‡] Michael Major,[‡] Barbara J. Kaboord,[‡] David Sarracino,[§] Taha Rezai,[§] Amol Prakash,[§] Mary Lopez,[§] Yongjie Ji,^{||} Waldemar Priebe,[‡] Frederick F. Lang,^{||} Howard Colman,^{||} and Charles A. Conrad^{||}

Pfizer Global Research and Development, 10770 Science Center Drive, San Diego, California 92121, Thermo Fisher Scientific, 3747 North Meridian Road, Rockford, Illinois 61101, Biomarker Research Initiatives in Mass Spectrometry (BRIMS), Thermo Fisher Scientific, 790 Memorial Drive Suite 201, Cambridge, Massachusetts 02139, and Department of Neuro-oncology and, Department of Experimental Therapeutics, M.D. Anderson Cancer Center, 1515 Holcombe Boulevard Unit 431, Houston, Texas 77030

Received September 5, 2009

Initiation and maintenance of several cancers including glioblastoma (GBM) may be driven by a small subset of cells called cancer stem cells (CSCs). CSCs may provide a repository of cells in tumor cell populations that are refractory to chemotherapeutic agents developed for the treatment of tumors. STAT3 is a key transcription factor associated with regulation of multiple stem cell types. Recently, a novel autocrine loop (IL-6/STAT3/HIF1 α) has been observed in multiple tumor types (pancreatic, prostate, lung, and colon). The objective of this study was to probe perturbations of this loop in a glioblastoma cancer stem cell line (GSC11) derived from a human tumor by use of a JAK2/STAT3 phosphorylation inhibitor (WP1193), IL-6 stimulation, and hypoxia. A quantitative phosphoproteomic approach that employed phosphoprotein enrichment, chemical tagging with isobaric tags, phosphopeptide enrichment, and tandem mass spectrometry in a high-resolution instrument was applied. A total of 3414 proteins were identified in this study. A rapid Western blotting technique (<1 h) was used to confirm alterations in key protein expression and phosphorylation levels observed in the mass spectrometric experiments. About 10% of the phosphoproteins were linked to the IL-6 pathway, and the majority of remaining proteins could be assigned to other interlinked networks. By multiple comparisons between the sample conditions, we observed expected changes and gained novel insights into the contribution of each factor to the IL6/STAT3/HIF1 α autocrine loop and the CSC response to perturbations by hypoxia, inhibition of STAT3 phosphorylation, and IL-6 stimulation.

Keywords: cancer stem cells • glioblastoma multiforme • quantitative phosphoproteomics • IL-6 • HIF1 α • STAT3 phosphorylation inhibition • LTQ-Orbitrap • LC-MS/MS • phosphopeptide enrichment • Western blot

Introduction

Many tumor types, including leukemia, breast, pancreas, prostate, head and neck, bone, colon, and brain, contain a small (<1%) subset of cells that are capable of initiating and maintaining tumors.^{1–24} Cells that demonstrate tumor-initiating properties are known as cancer stem cells. Cancer stem cells (CSCs) are hypothesized to provide a repository of cells in

tumor cell populations that are refractory to radiation and chemotherapeutic agents developed for the treatment of tumors.²⁵ The potential lack of response of CSCs to traditional cytotoxic and radiation therapies has significant implications for tumor biology and therapeutics. Thus, knowledge of CSC signaling pathways involved in the maintenance of tumor stem cells may yield new therapeutic targets that could increase the efficacy of cancer treatments.

The identification of cancer stem cells relies on a functional definition and expression of molecular markers. A tumor stem cell must be able to both initiate tumors and give rise to the heterogeneous cell types observed in the parent tumor from which the CSCs are derived. Functional evaluation of both self-renewal and tumor propagation is evaluated by assays of self-renewal *in vitro* and serial transplantation of tumor cells *in vivo*.²⁶ In the case of human brain tumors, the characterization

* To whom correspondence should be addressed. Carol L. Nilsson, Pfizer Global Research and Development, 10770 Science Center Dr., San Diego, CA 92121. Phone: (858) 622-7371. FAX: (858) 678-8164. E-mail: Carol.Nilsson@pfizer.com.

† Pfizer Global Research and Development.

‡ Thermo Fisher Scientific.

§ Biomarker Research Initiatives in Mass Spectrometry.

|| Department of Neuro-oncology, M.D. Anderson Cancer Center.

‡ Department of Experimental Therapeutics, M.D. Anderson Cancer Center.

Neurosphere Assay

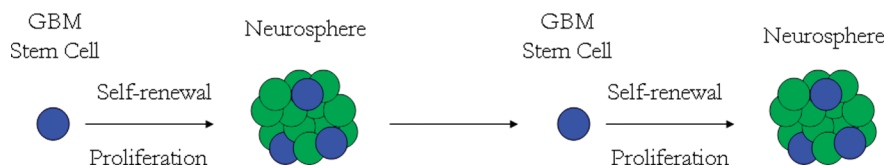


Figure 1. In the neurosphere assay, tissues are broken down into single cells, which are then cultured in serum-free medium. True stem cells in the culture grow and divide, forming clusters of cells called neurospheres.

WP1193

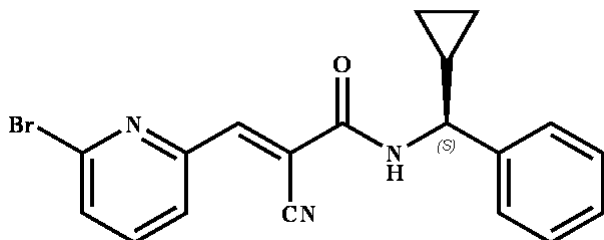


Figure 2. Chemical structure of the small molecule inhibitor of STAT3 phosphorylation by JAK2 (WP1193) used in this study.

of putative cancer stem cells benefits from use of the neurosphere assay, originally used to isolate normal embryonic stem cells from the central nervous system.^{27,28} In the neurosphere assay (Figure 1), tissues are broken down into single cells, which are then cultured in serum-free medium supplemented with epidermal growth factor (EGF) and basic fibroblast growth factor (bFGF). Stem cells in the culture grow and divide forming clusters of cells called neurospheres. Cancer stem cells from glioma samples form neurospheres²⁹ and express some markers also expressed by normal stem cells from embryonic brain, such as CD133, nestin and glial fibrillary acidic protein (GFAP). In particular, CSCs that express CD133 show enhanced ability for self-renewal as neurospheres and for tumor initiation.¹⁹

Several glioblastoma cancer stem cell (GSC) lines have been isolated from primary and recurrent tumors from patients treated at M.D. Anderson Cancer Center in Houston, Texas. These cell lines form neurospheres and demonstrate the ability to express multiple lineage markers and reliably form tumors that recapitulate many of the pathological features of the original tumors after intracranial xenograft.³⁰ Prior studies have demonstrated that STAT3 is constitutively activated in GSCs maintained as neurospheres and that blockade of STAT3 activation in GSCs by the novel JAK2/STAT3 phosphorylation inhibitor WP1193 (Figure 2) results in blockade of self-renewal and proliferation of GSCs.³¹ In 2007, a novel autocrine loop (IL-6/STAT3/HIF1 α) was discovered in pancreatic cancer cells (Figure 3).³² IL-6 induces the JAK2 pathway via the IL-6 receptor and STAT3 is a downstream target that is phosphorylated and becomes an activated dimer.³³ Activated STAT3 increases HIF1 α (induced by hypoxia) by blocking degradation or enhancing synthesis.³⁴

The signal transduction and activator of transcription (STAT) proteins regulate many key cellular and cancer functions, such as cell cycle progression, apoptosis, tumor angiogenesis, immune surveillance, invasion and metastasis.³⁵ Regulation of those functions is performed by STAT phosphorylation by receptor tyrosine kinases, Src, Bcr and Janus kinases (JAKs). Activation of STAT proteins is typically transient in normal cells, but in tumors, constitutive activation of STAT3 or STAT5 is

The IL-6/STAT3/HIF1 α Autocrine Signaling Loop

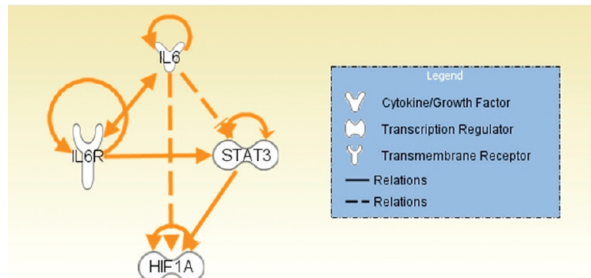


Figure 3. Pathway model produced by Ingenuity Systems that shows the interaction between IL-6 (IL6) and its receptor (IL6R), STAT3 and HIF1 α (induced by hypoxia). Solid lines indicate a direct interaction and dotted lines show an indirect interaction between the proteins. Interference of human STAT3 mRNA by siRNA decreases expression of human HIF1 α protein that is increased by IL-6.³⁸

widespread. Activated STAT3 increases the secretion of inflammatory cytokines such as VEGF, IL-6 and IL-10,³⁶ and those cytokines increase STAT3 activation primarily via JAK2. Small molecule inhibitors of STAT3 phosphorylation have been reported to be efficacious in glioblastoma therapy in animal models.³⁷ IL-6 is also elevated in many cancers³³ and is a potential regulator of stem cell renewal^{38,39} and proliferation.⁴⁰

The contribution of oxygen concentration to protein expression in CSC culture is relevant because the cells are hypothesized to maintain a stem-like character more readily in a hypoxic environment. Typically, cell cultures are kept in an atmosphere that contains 20% O₂; however, oxygen concentration is 5–10% in the brain and 0.1–10% in glioblastoma tumors. A recent study of gene expression and embryonic marker expression in GSC11 and other glioma CSC lines demonstrated that a larger number of transcripts were affected in CSC lines than mature glioma cell lines in hypoxia (7% O₂).⁴¹ Nestin, CD133 and SOX2 expression were increased in CSCs in hypoxia and those cells demonstrated an increased proliferation rate and self-renewal potential. Cellular responses to hypoxia are mediated by hypoxia-inducible factors (HIFs)⁴² and studies have shown that HIF1 α knockdown by siRNA decreases IL-6 production.⁴³

Global phosphoproteomic analysis, especially when performed in a quantitative fashion, can provide a powerful analytical tool to study intracellular signaling pathways activated by internal or external cellular stimuli.^{44–49} Mass spectrometry based methods have provided comprehensive phosphoprotein measurements in biological systems.^{46,48,50–53} Furthermore, the use of isotopically enriched mass tags allows protein assays to be multiplexed⁵⁴ and considerably reduces the time needed to acquire data because it eliminates the need to compare multiple LC/MS/MS data sets. Experimental reports in which TMT reagents were used to study the proteomes of

Phospho-enrichment and Quantification Workflow

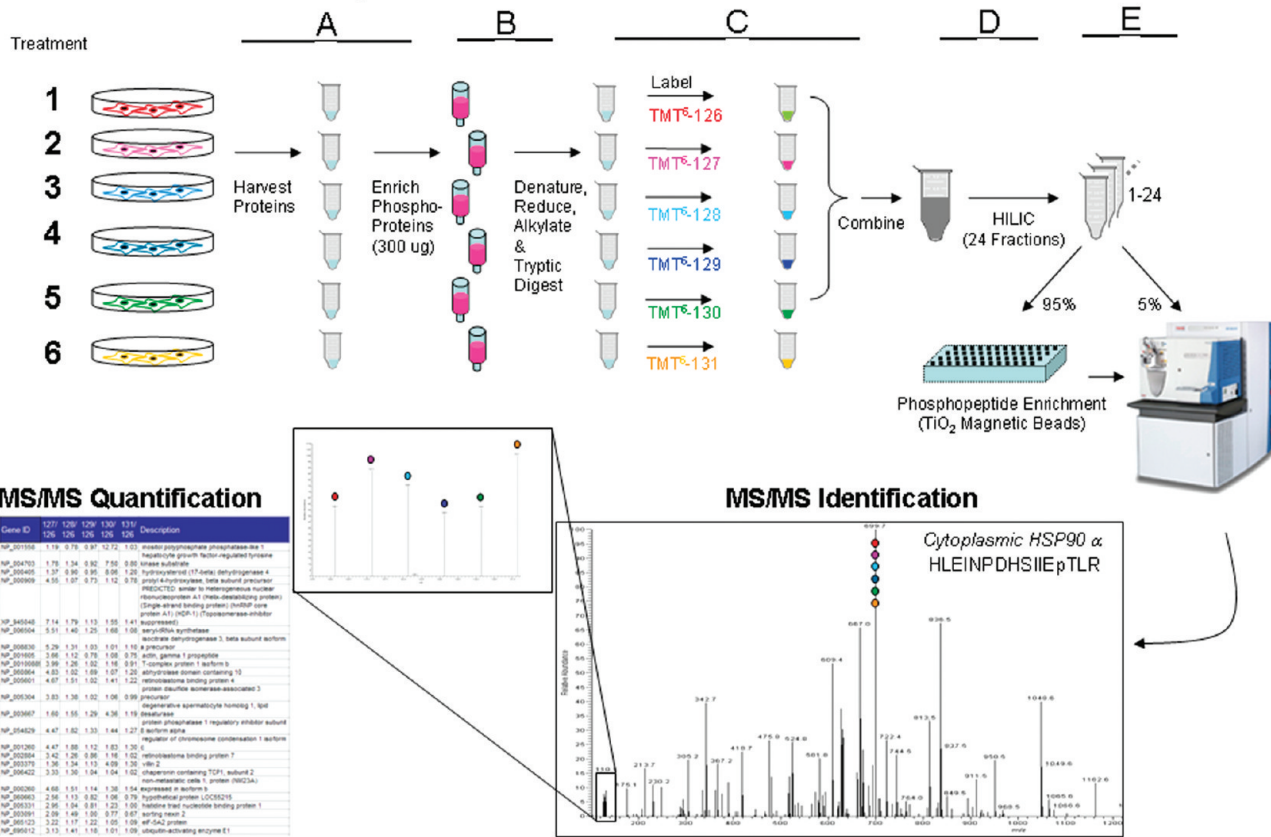


Figure 4. Outline of the quantitative phosphoproteomic workflow developed for phosphoprotein and phosphopeptide quantitation in treated GSC11 cells. The six GSC11 treatments were 1, normoxic control; 2, hypoxic control; 3, WP1193 in normoxia; 4, WP1193 in hypoxia; 5, WP1193 and IL-6 stimulation in normoxia; and 6, WP1193 and IL-6 stimulation in hypoxia. The workflow included phosphoprotein enrichment, chemical modification of tryptic peptides with isobaric TMT tags, enrichment by HILIC chromatography and TiO₂ beads, followed by LC–MS/MS in an LTQ-Orbitrap.

human cerebrospinal fluid⁵⁵ and *Neisseria meningitidis*⁵⁶ have been published recently.

We developed a novel quantitative phosphoproteomic approach to measure GSC11 responses to STAT3 phosphorylation inhibition by WP1193 treatment and IL-6 stimulation under normoxic and hypoxic conditions. The workflow included phosphoprotein enrichment of cell lysates from six treatment conditions, in-solution digestion, chemical labeling of peptides with isobaric mass tags, HILIC fractionation,⁵⁷⁻⁵⁹ phosphopeptide enrichment by use of TiO₂ magnetic beads, and LC-MS/MS in a ThermoScientific LTQ-Orbitrap instrument (Figure 4). Quantitative data sets were further analyzed by a pathway analysis tool to gain insight into the relative contribution of each stimulus to the regulation of phosphoprotein signaling. Verification of up- and down-regulation of seven proteins was provided by a rapid Western blot technique. Additionally, the basal secretion of nine pro-inflammatory cytokines by GSC11 cells in normoxia and hypoxia was measured.

Experimental Section

The experiments described below were performed twice, once with a single culture plate of each treatment and the second time with lysates from three plates to obtain better coverage of the cells' proteome (>3000 proteins in the second experiment versus ~300 in the first). Because the experimental methods differed between the biological experiments, we did

not combine the results but rather show results from the second study only.

Cell Culture Conditions and Treatments. GSC11 cells were cultured in 150 mm dishes in DMEM/F12 (1:1) media supplemented with B27 (Invitrogen, Carlsbad, CA), EGF (Sigma, St. Louis, MO) and bFGF (Sigma). Cells were incubated at 37 °C and 5% CO₂ and 20% O₂ (normoxia) or 1% O₂ (hypoxia). Basal secretion levels of IL-6 and other cytokines (hGM-CSF, IFN-γ, IL-10, IL-12p70, IL-1β, IL-2, IL-8, and TNFα) by GSC11 cells in surrounding media in normoxia and hypoxia were assessed by measurement in a Mesoscale 2400 imager. Normoxic and hypoxic cells ($\sim 1 \times 10^7$) were treated with vehicle control (DMSO), STAT3 phosphorylation inhibitor (WP1193,³⁷ 5 μM) or WP1193 plus IL-6 stimulation (Biosource, Camarillo, CA, 10 ng/mL). Each treatment was performed for 24 h, with the exception of IL-6 stimulation, which added 20 min prior to cell lysis.

Cells from three separate culture plates per treatment were centrifuged at $240 \times g$ for 5 min (4°C) and washed twice with 50 mM HEPES (pH 7.0). Cells were lysed with modified RIPA buffer (150 mM NaCl, 50 mM Tris-HCl, pH 7.4; 1% NP-40, 0.25% sodium deoxycholate, 1 mM EDTA) mixed with inhibitors (Thermo Scientific Halt protease inhibitor EDTA-free and Halt phosphatase inhibitor cocktail, Thermo Fisher Scientific, Rockford, IL) and incubated on ice for 15 min. Lysis was completed by ultrasonication in 5–8 s pulses. Cell lysates were centrifuged

at $15\,000\times g$ for 20 min ($4\text{ }^{\circ}\text{C}$) to remove cellular debris. Supernatants were stored at $-80\text{ }^{\circ}\text{C}$ until phosphoprotein enrichment.

Phosphoprotein Enrichment. Following cell lysis, proteins were enriched in a phosphoprotein enrichment column (Thermo Scientific Phosphoprotein Enrichment Kit, Thermo Fisher Scientific, Rockford, IL), exactly according to the manufacturer's instructions. In short, 3.5 mg of protein from each GSC11 cell lysate was applied to a phosphoprotein column that contained a proprietary enrichment gel and buffer. The samples were incubated in the column for 30 min at $4\text{ }^{\circ}\text{C}$ and washed with lysis/binding/wash buffer provided in the kit to remove unbound proteins. Bound proteins were eluted with five column washes of elution buffer provided in the kit. The phosphoprotein yields, typically between 15–25% of the total protein loaded, were determined using the Bradford assay.⁶⁰ Phosphoprotein-enriched samples were stored at $-80\text{ }^{\circ}\text{C}$.

Tandem Mass Tag (TMT) Technology. Each sample (100 μg protein in triplicate) was adjusted to give a final volume of 100 μL with 45 μL 200 mM tetraethylammonium bromide (TEAB) and water (as necessary). Five microliters of 200 mM *tris*(2-carboxyethyl)phosphine (TCEP) buffered with TEAB was added to each sample (final TCEP concentration was 10 mM) and incubated at $55\text{ }^{\circ}\text{C}$ for 1 h. Five microliters of 375 mM iodoacetamide (buffered with TEAB) was added and incubated in the dark for 30 min. Proteins were precipitated in four volumes (440 μL) of ice cold acetone for 2 h at $-20\text{ }^{\circ}\text{C}$. Samples were centrifuged at $10\,000\times g$ for 30 min ($4\text{ }^{\circ}\text{C}$) after which the supernatants were removed and discarded. Pellets were air-dried and resuspended in 12.5 μL of 8 M urea. Trypsin (10 μg in 87.5 μL of TEAB buffer) was added, and the samples were incubated for 24 h at $37\text{ }^{\circ}\text{C}$. Each sample was tagged by use of a Thermo Scientific TMTsixplex Isobaric Mass Tagging Kit (Thermo Fisher Scientific, Rockford, IL) according to the manufacturer's instructions. The chemically tagged samples were combined into one tube and stored at $-80\text{ }^{\circ}\text{C}$.

HILIC Fractionation and Phosphopeptide Enrichment. C18 solid-phase extraction (SPE) media (Thermo Scientific HyperSep SPE Columns, Thermo-Fisher Scientific, Bellefonte, PA) was used to desalt the digested samples, adapted for single use by centrifugation ($500\times g$ for 3–5 min). The centrifugation conditions were adjusted to achieve a processing time of 0.5–1 min residence time in the media bed. The C18 resin was conditioned before use by filling the SPE device with acetonitrile and allowing the solvent to pass through the media slowly (1–2 min). This process was repeated twice. The resin was rinsed three times with 0.25% (v/v in water) trifluoroacetic acid (TFA). The TMT-labeled sample was loaded and flowed over the resin by centrifugation for a residence time of 0.5–1 min and washed four times with 0.25% TFA. Finally, the desalted sample was eluted with 1 mL of 80% acetonitrile/0.1% formic acid (aqueous) by centrifugation. Samples were frozen, lyophilized to dryness and reconstituted in 1.3 mL of 85% acetonitrile/56 mM formic acid (aqueous), pH 3.0. Samples were fractionated by using a hydrophilic interaction chromatography column (HILIC, PolyLC PolyHydroxyethyl A, PolyLC Inc., Columbia, MD), 200 \times 4.6 mm, particle size 5 μm . Buffer A was 85% acetonitrile/56 mM formic acid, pH 3.0 and Buffer B was 8.5 mM ammonium formate/56 mM formic acid, pH 3.0. Twenty-four 1 mL fractions were collected according to the following gradient: equilibrate with ten column volumes of 100% A, load sample, wash unbound sample with four column volumes of 100% A,

begin sample collection with 3.5 column volumes to 15% B, four column volumes to 40% B and finally 10 column volumes to 100% B.

All fractions were lyophilized to dryness, then reconstituted in 150 μL of 80% acetonitrile/2% formic acid (aqueous). Ninety-five percent of each sample was phosphopeptide-enriched by use of TiO₂ beads and a robotic system (Thermo Scientific KingFisher Flex Purification System, Thermo Scientific and Magnetic TiO₂ Phosphopeptide Enrichment Kit, Pierce). The Phosphopeptide Enrichment PCR Plate protocol, available for download from the Thermo Scientific KingFisher Web site (www.thermo.com/kingfisher), a purification system with a PCR magnet head (KingFisher Flex) and a 96 tip comb for PCR magnets (KingFisher Flex) were used for this application. Preparation of buffers, TiO₂ beads and enrichment on the purification system were performed according to the manufacturer's instructions. All plastic 96-well plates were rinsed three times with acetonitrile to minimize contamination from polymers leaching from the plastics. The TiO₂ magnetic beads were placed into a 15 mL polypropylene conical tube and mixed thoroughly by repeated inversion. Prepared binding buffer was added to the bead suspension (140 μL binding buffer per 10 μL of resin) and samples were processed according to the manufacturer's instruction, then transferred to clean 0.2 mL PCR plates (Thermo Scientific) and lyophilized to dryness.

High Resolution LC–MS/MS. Samples were rehydrated in 5% (v/v) acetonitrile/1% (v/v) formic acid in water and injected with an autosampler (Thermo Scientific MicroAutosampler) on a 75 μm \times 25 cm fused silica capillary column packed with C18 media (Thermo Scientific Hypersil GOLD Column, 5 μm), in a 250 $\mu\text{L}/\text{min}$ (1000:1 split to column) gradient of 5–30% (v/v) acetonitrile, 0.2% (v/v) formic acid for 180 min (total LC run time of 240 min). The LTQ-Orbitrap was operated in a top 4 configuration at 60 000 resolving power (defined by $m/\Delta m 50\%$) for a full scan, with monoisotopic precursor selection enabled, and +1, and unassigned charge states rejected. Fragmentation of ions was achieved with higher energy collisional dissociation (HCD) fragmentation^{61,62} at 15 000 resolving power in the LTQ-Orbitrap using an isolation window of 4.5, collision energy of 45, default charge state of 4 and activation time of 30 ms.

Fast Western Blots. Following SDS-PAGE of lysates from treated and control GSC11 cells, proteins were transferred from gels to PVDF membranes using the Thermo Scientific Pierce Fast Transfer System (Pierce Fast Transfer Buffer, Pierce Fast Semi-Dry Blotter, Thermo Fisher Scientific, Rockford, IL). One membrane was simultaneously probed for STAT3 and phospho-STAT3 followed by dual channel fluorescent detection (Thermo Scientific DyLight 680- and DyLight 800- conjugated secondary antibodies, Thermo Fisher Scientific, Rockford, IL). A separate membrane was probed for cyclophilin B followed by dual channel fluorescent detection (DyLight 680- and DyLight 800- conjugated secondary antibodies, Thermo Fisher Scientific, Inc.). Four different membranes were separately probed for GFAP, HIF1 α , HIF2 α and inducible NO-synthase (iNOS), using the Thermo Scientific Pierce Fast Western Blot Kit and chemiluminescent detection (Thermo Fisher Scientific, Rockford, IL).

Data Analysis, Informatic Searches and Pathway Analysis. LC–MS/MS data analysis was performed with Thermo Scientific BioWorks 3.3.1 and the human IPI database (version 55). Peptides and proteins identifications were filtered with a DeltaCN = 0.1 and charge state dependent Xcorr values ($z = 1$: 1.9, $z = 2$: 2.5, $z = 3$: 3.5) requiring at least two peptides

per protein. The filters allowed a 95% confidence level of protein identification (5% false discovery rate). The PepQuan function in Bioworks was used to quantify the TMT reporter ion intensities at 126.13–131.14 *m/z*. Protein identification and quantitation intensity ratios were exported to Microsoft Excel software. Reporter ion isotope correction factors were applied by subtracting the contribution of reporter ion isotopes to adjacent reporter ion intensities and adding these intensities back to the proper channel, after which data were normalized by median intensities for subsequent analyses. A confidence interval of 1.3-fold or greater change was determined to be significant by using alpha = 0.01 with a Bonferroni correction⁶³ for the number of proteins quantified in the five ratio conditions. Gene ontologies of identified and quantified proteins were determined with Inforsense software (Inforsense Ltd., www.inforsense.com).

Normalized quantitative data sets were analyzed by use of Ingenuity Pathways Analysis (Ingenuity Systems, version 7.6 (www.ingenuity.com)). The data set contained protein identifiers and TMT reporter ion ratios normalized to either the normoxic or hypoxic control values. A 1.5-fold cutoff value was set to identify proteins whose expression was significantly increased or decreased. Ingenuity Pathway Analysis software protein networks were created using proteins with 1.5-fold or greater changes in expression upon treatment and molecular interactions described in the scientific literature. Networks represent a highly interconnected set of proteins derived from the input data set. Biological functions and processes were attributed to networks by mapping the proteins in the network to functions in the Ingenuity ontology and performing a right-tailed Fisher's exact test to determine the significance (*p*-value) of any overrepresentation of proteins to a function compared to the result expected by a random set of proteins. Top ranked biological functions are those with the lowest *p*-values. A similar calculation was done to assign biological functions to the entire data set of overexpressed proteins. To predict which pathways are being affected by the changes in protein expression, a Fisher's exact test was applied to the mapping of significantly over- and under-expressed proteins in the data set to each pathway to determine the significance of any overrepresentation of the proteins to that pathway.

Results and Discussion

Western Blots and Chemokine Secretion. The baseline secretion of cytokines by GSC11 cells has not been studied previously. Because our experimental design included stimulation of the cells by IL-6 and hypoxia, we determined the level of pro-inflammatory cytokine secretion by cells cultured in normoxic and hypoxic conditions (Figure 5). IL-6 and several other cytokines (hGM-CSF, IFN γ , IL-10, IL-12p70, IL-1 β , IL-2, and TNF α) were secreted into cell media at low levels (<6 pg/mL) and hypoxic treatment decreased the levels further. We deemed the endogenous production of IL-6 by GSC11 cells to be negligible in comparison to the amount of exogenous IL-6 added to cell cultures during stimulation (10 ng/mL). In contrast to the other cytokines, IL-8 secretion was more than doubled in hypoxia. IL-8 is a proangiogenic chemokine that is highly expressed in gliomas *in vitro* and *in vivo*, with the highest expression in necrotic (hypoxic) areas of tumors.⁶⁴

We also studied, by Western blot (Figure 6), the expression of seven proteins that were relevant to the experimental design and the quantitative phosphoprotein results obtained by LC–MS/MS analysis. The response of STAT3 and Tyr705

Secretion of Cytokines by GSC11 Cells in Normoxic and Hypoxic Conditions

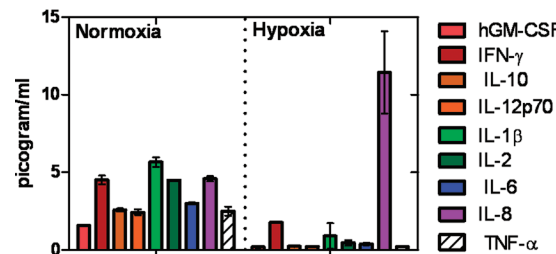


Figure 5. Basal levels of pro-inflammatory cytokine secretion by GSC11 cells cultured under normoxic and hypoxic conditions were assessed by mesoscale detection. Cytokine levels were measured in tissue culture medium by a Mesoscale 2400 imager. Results represent means and standard errors of the means from duplicate cultures. The expression of most cytokines, including IL-6, is low in normoxic cells and decreases further in hypoxia; however, IL-8 secretion shows the opposite trend.

Fast Western Blot of Key Proteins in GSC11

	Lane 1	Lane 2	Lane 3	Lane 4	Lane 5	Lane 6
Norm/Hyp	Nor	Hyp	Nor	Hyp	Nor	Hyp
STAT-3 1nt	-	-	+	+	+	+
IL-6	-	-	-	-	+	+

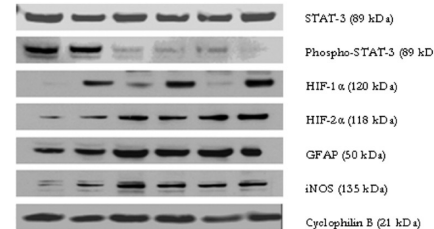
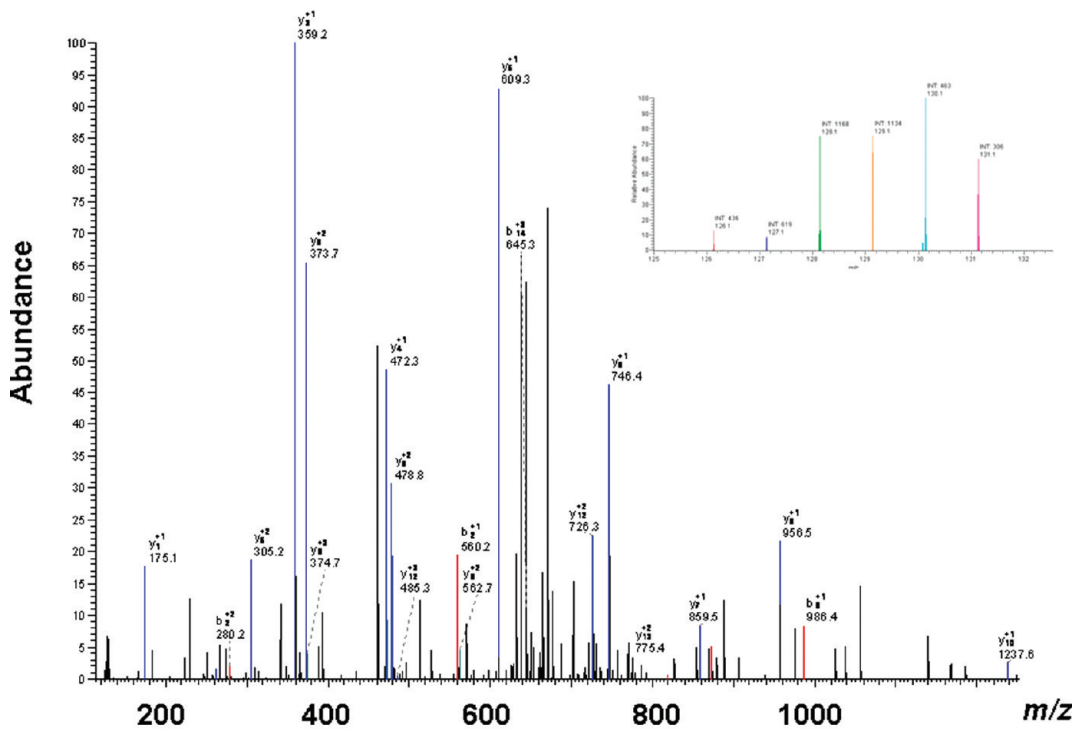


Figure 6. Expression of seven proteins relevant to the experimental design and MS results was quantitated by Western blot. As expected, phosphorylated STAT3 decreased in response to WP1193 treatment, regardless of IL-6 addition or oxygen concentration. HIF1 α expression was increased by hypoxia, and HIF2 α was increased by all treatments. Cyclophilin B was chosen as a control protein.

phosphorylated STAT3 followed the expected pattern. Total STAT3 levels were not reduced by WP1193 treatment; however, the addition of WP1193 greatly decreased phosphorylated STAT3 levels, irrespective of oxygen concentration or IL-6 addition. HIF1 α was increased by hypoxic conditions, but also by the addition of WP1193, a STAT3 phosphorylation inhibitor, to normoxic cells. Based on the known relationship of STAT3 to HIF1 α a decrease of HIF1 α would be expected by inhibition of STAT3 phosphorylation.³⁴ However, pathway analysis by use of Ingenuity Systems showed that EGF signaling was increased in WP1193-treated cells. EGF has been previously observed to increase HIF1 α expression in MDA MB231 and MCF7 cells as determined by immunoblot studies.⁶⁵ Cross-talk between the EGF and HIF1 α signaling was observed in those cell lines and may represent a mechanism of resistance to apoptosis. The expression of HIF2 α , the regulation of which differs from HIF1 α in glioma stem cells,⁶⁶ was increased by all treatments relative to the normoxic control.

Identification of Phosphoproteins and Phosphopeptides. Enrichment of the phosphoproteome yielded 3414 nonredundant protein assignments (Supplementary Table 1, Supporting Information). Approximately 4000 phosphopeptide assignments were made. Tandem mass spectra from TMT-tagged peptides

**A BCLAF1 BCL-associated Transcription Factor
pYSPSQNpSPIHHIPSR**



**B PPID 40 kDa Peptidyl-prolyl *cis-trans* isomerase
DGSGDSHPDFPEDADIDLK**

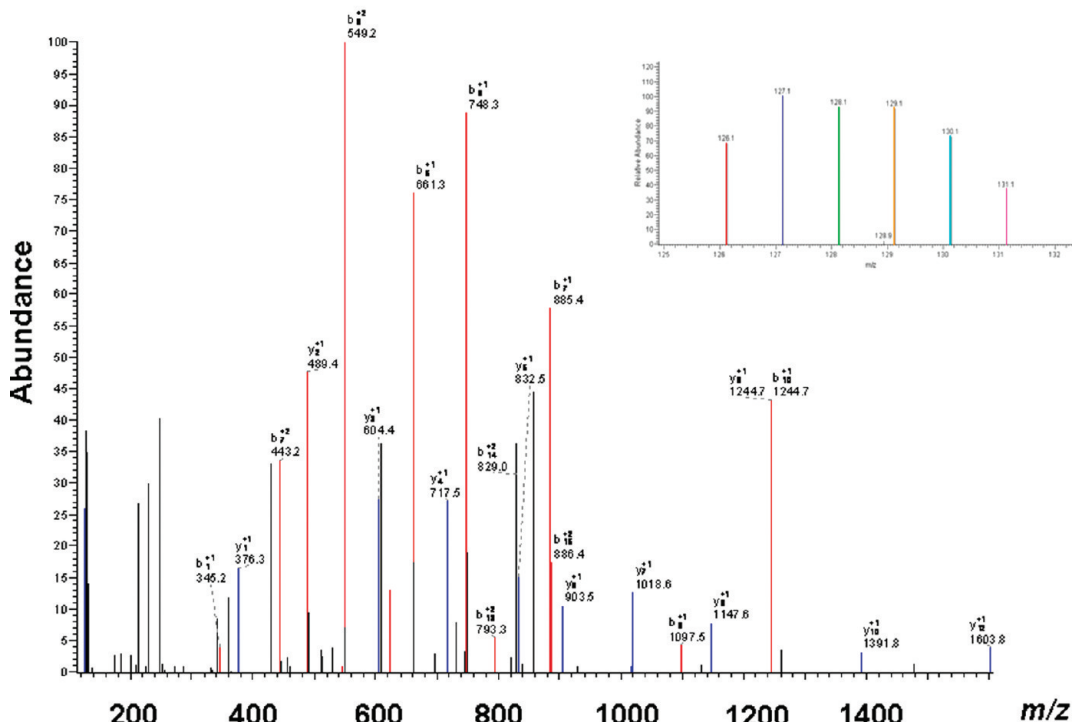


Figure 7. (A) Tandem mass spectrum of a phosphopeptide from BCL2-associated transcription factor. The abundance of b - and y -ions allows for confident assignment of the peptide's identity. Inset: reporter ions used for quantitation are magnified and indicate quantitative changes in this measured peptide by treatment with WP1193 and IL-6. (B) Tandem mass spectrum from a peptidyl-prolyl *cis-trans* isomerase. In this case, the reporter ions (inset) indicate no significant quantitative change by the various treatments.

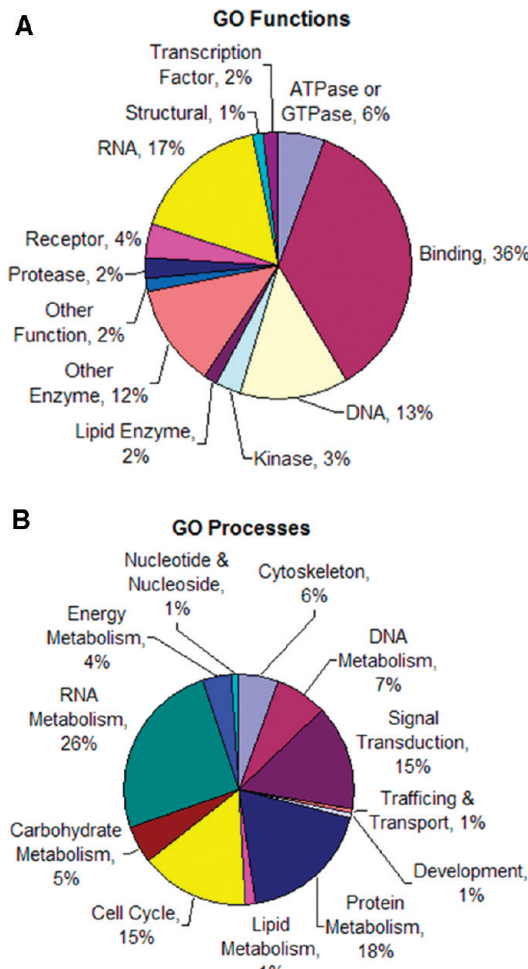


Figure 8. Assignments of gene ontology (A) functions and (B) processes associated with proteins changed 1.5-fold or greater in the phosphoproteomic data set.

yielded abundant *b*- and *y*-type ions for peptide identification as well as “reporter” ions of nominal mass 126–131 for quantitation of peptide abundances derived from the various treatments (Figure 7A, B). The large number of protein identifications was enhanced by merging data from protein digest samples enriched by HILIC fractionation only (2341 proteins) and the combination of HILIC and TiO₂-enrichment (1895 proteins). Analysis of the GO functions and processes of proteins whose expression changed 1.5-fold or more (Figure 8A, B) indicated that key categories of proteins were enriched in our data set, including those related to signal transduction, cell cycle control, kinases, enzymes, and transcription factors.

Potential Interference of Tryptophan in TMT6 Quantitation. During the method development process, we observed that some tryptophan-containing peptides produced an ion in the TMT6 reporter ion region that can potentially cause interference in quantitation in the 130 channel (mass 130.142), as well as (but to a lesser extent) the 131 channel (mass 131.139, Figure 9). The ion (mass 130.066) was assigned as a fragment of the tryptophan immonium ion. The interfering ion’s intensity is higher under conditions that produce more tryptophan immonium ions, such as higher charge states. The solution to this potential interference requires both the mass spectrometer to have resolving power better than >4000 at *m/z* 130, and the data processing software to be able to distinguish

contributions from the tryptophan fragment. Recently, similar observations of immonium ion interference were made in a related quantitation approach (iTRAQ).⁶⁷

Protein Identification and Pathway Analysis. Of the proteins whose expression changed more than 1.5-fold, twenty-one proteins were linked directly or indirectly to the STAT3, HIF1α or IL-6/IL-6R as determined by Ingenuity Pathway analysis (Table 1). The following sections describe the relationships of proteins to canonical pathways and interlinked networks that were affected by treatments. The data set can be examined from many angles. Some valid comparisons to perform are the effect of hypoxia, the effect of WP1193 treatment on hypoxic or normoxic cells, and the effect of WP1193 treatment and IL-6 on hypoxic or normoxic cells.

Effect of Hypoxia on GSC11 Cells. Relative changes in phosphoprotein ratios were determined by comparison of the hypoxic and normoxic control samples (Supplementary Table 2, Supporting Information). Fifteen canonical signaling pathways were impacted as determined by Ingenuity analysis. Pathways identified with a p-value less than 0.05, determined by the number of proteins in the quantitative phosphoproteomic data set compared to the number of proteins that participate in a particular pathway, may reflect which pathways overlap the most with the proteins quantified. In hypoxia, the pathways included carbohydrate metabolism, inositol phosphate metabolism, phosphatase and tensin homologue (PTEN) and HIF1α signaling. The cellular response to hypoxia by metabolic changes is well-known and expected.⁶⁸ Eleven proteins known to interact with HIF1α were identified in this assay (Table 1). Four molecules directly involved in the HIF1α signaling pathway were increased, including APEX1, ARD1A, EGLN1 and MAPK1. Egl nine homologue 1 (EGLN1) regulates HIF1α by hydroxylation⁶⁹ and is associated with VEGF expression⁷⁰ (also regulated by ARD1A, which acetylates both HIF1α and VEGF). APEX nuclelease (APEX1) is a cytosolic enzyme involved in both HIF1α signaling and inositol metabolism and regulates TP53⁷¹ in addition to HIF1α. An increase in expression of APEX1 has been associated with survival of germ cell tumor lines during radiation and chemotherapy.⁷² Other HIF1α-interacting proteins in this set included upregulated procollagen-lysine, 2-oxoglutarate 5-dioxygenase 2 (PLOD2), mitogen-activated protein kinase 1 (MAPK1) and N-myc downstream-regulated 1 (NDRG1), all known to be increased by HIF1α activity. One factor that increases HIF1α degradation was found to be increased, glycogen synthase kinase 3β (GSK3B).⁷³

Because HIF2α was recently implicated in the hypoxic response of glioma stem cells,⁴² we examined the relationship of the quantitated proteins to HIF2α by use of Ingenuity Pathway Analysis. We found six proteins related to HIF2α, about half the number of protein findings related to HIF1α. Of the proteins that were increased or decreased, there was complete overlap with the relationship findings for HIF2α when compared to HIF1α. Our interpretation of this result is that less knowledge has been published surrounding HIF2α, and that further study is needed to determine the exact contribution of each hypoxia-induced factor to the hypoxic response of GSC11 and other glioma stem cells. Also, the different patterns of response by HIF1α and HIF2α to the treatments, as studied by Western blot (Figure 6), reinforce the need for deeper examination of the proteins’ mechanism of response in GSC11 cells.

Four molecules in the PTEN pathway were changed by the effect of hypoxia, including GSK3B, membrane-associated

Tryptophan Fragment in TMT6 Reporter Ion Region

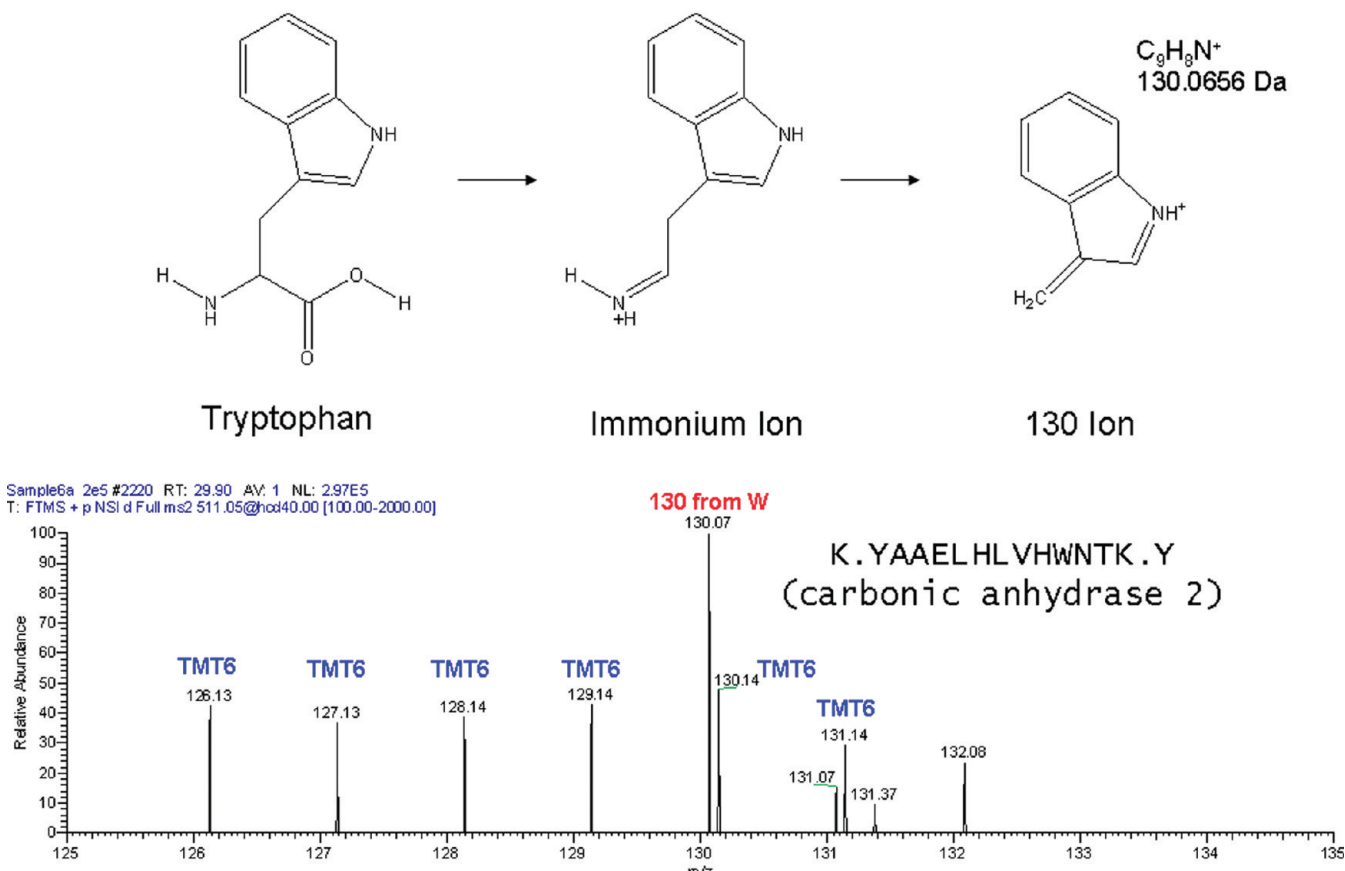


Figure 9. Potential interference from the immonium ion fragment derived from tryptophan in TMT quantitation can be avoided successfully by use of a mass analyzer with a resolving power greater than 4000 at m/z 130.

Table 1. Proteins Identified and Quantitatively Regulated 1.5-Fold or Higher in the MS Data Set That Interact Directly with STAT3, HIF1 α , IL-6 and its Receptor

HIF1 α	STAT3	IL-6
APEX1	APEX1	ANXA1
ARD1A	CSK	CSK
EGLN1	GNB2L1	FSTL1
GNB2L1	GSK3B	GSK3B
HIST1H1C	GTF2I	HMGB1
MAPK1	KRT1	HSP90B1
NDRG1	MAP2K1	LIG1
P4HA1	MAPK1	MAP2K1
PLOD2	MAPK1	
PPIA		
TFRC		

guanylate kinase (MAGI1), mitogen-activated protein kinase kinase 1 (MAPKK1) and MAPK1. The effect on the PTEN pathway is of interest because loss of PTEN or reduced activity is frequently associated with glioblastomas.⁷⁴ The increased activation of the PTEN pathway in hypoxia may result in decreased cell migration and spreading of those cells relative to normoxic GSC11 cells. One proposed biomarker of PTEN activity in glioblastoma multiforme, IGFBP2,⁷⁵ was also increased 1.4-fold in the hypoxic cells.

The proteins most increased by hypoxic growth conditions were erythrocyte membrane protein band 4.1-like 1 (EPB41L1) and HSP90 (Supplementary Table 2, Supporting Information).

EPB41L1 is a multifunctional protein enriched in neurons and embryonic cell lines^{76,77} that mediates cell membrane-cytoskeletal interactions and is involved in G1 phase of the cell cycle.⁷⁸ HSP90 is a direct interacting partner of the HIF1 α /STAT3/IL-6 feedback loop. The two most decreased proteins were two cytoskeletal components, annexin A1 (ANXA1) and fascin 1 (FSCN1).

Ingenuity Pathway Analysis software protein networks were created using proteins changed 1.5-fold or greater in hypoxic growth conditions and molecular interactions based on scientific literature evidence. Of the cellular network functions that were changed significantly, RNA post-transcriptional regulation, cell assembly and organization and gene expression in cellular compromise were the most highly modulated (Supplementary Table 2, Supporting Information). Taken together, the effect of hypoxic cell culture conditions on GSC11 cells appears to activate the networks and pathways associated with hypoxia in other cells. Because the hypoxic response of CSCs is associated with resistance to apoptosis, close investigation of proteins regulated in the CSC response may yield new therapeutic targets.

Effect of STAT3 Phosphorylation Inhibition in Normoxic GSC11 Cells. As determined by Ingenuity Pathways Analysis, the top network functions associated with WP1193 treatment were protein synthesis, RNA post-transcriptional modification and cell cycle. Proteins affected by WP1193 treatment showed a statistically significant ($p < 0.05$) over-represented mapped

proportion to more than twenty signaling pathways compared to proportions expected from a random set of proteins, including the VEGF, apoptosis, retinoic acid receptor (RAR), tight junction signaling, and OKT4 in mammalian embryonic stem cell pluripotency pathways (Supplementary Table 3, Supporting Information). Within the VEGF pathway, embryonic lethal, abnormal vision-like 1 (ELAVL1) was increased 2-fold. ELAVL1 is expressed in glioblastoma cell lines and is one regulator of STAT3 expression.⁷⁹ PARP1, a member of the apoptosis, RAR and OKT4 pathways increased 1.6-fold by WP1193 treatment. Poly(ADP-ribosyl)transferase 1 (PARP1) is a chromatin-associated enzyme that modifies various nuclear proteins by poly(ADP-ribosyl)ation. The modification is dependent on DNA and is involved in the regulation of various important cellular processes such as differentiation, proliferation, tumor transformation, and regulation of the molecular events involved in the recovery of cells from DNA damage.

The effect of WP1193 on polar lipid and glycogene expression of GSC11 cells was recently studied.⁸⁰ It was determined by mass spectrometric analysis that STAT3 phosphorylation decreased the expression of several gangliosides, including GM1 and GD1. Also, sialidase 1 expression was decreased as determined in a transcriptomic assay. In our study, we found three enzymes related to N-glycan synthesis to be increased, GANAB, RPN1 and STT3B, results which are consistent with the lipidomic findings. Also, an enzyme related to glycolipid degradation, HEXB, was determined to be modulated by WP1193 treatment. One of the most increased proteins in the phosphoproteomic data set was ANK2, a protein expressed in embryonic tissues⁸¹ but not detected in differentiated brain cancer cells.⁸² ANK2 binds to the membrane glycoproteins CD44 and L1CAM, which bear a sulfated glycoepitope found to be expressed in GSC11 cells in the lipidomic study. Because GSC11 cells release from neurospheres in WP1193 treatment, modulation of molecules related to cell–cell adhesion (glycolipids and glycoproteins) are expected.

Effect of STAT3 Phosphorylation Inhibition in Hypoxic GSC11 Cells. The effect of WP1193 treatment of GSC11 cells in a hypoxic environment elicited a different response compared to WP1193 treatment in normoxia. The top networks associated with the hypoxic data set were amino acid, drug and carbohydrate metabolism (Supplementary Table 4, Supporting Information). Pathways involved in carbohydrate metabolism were more highly modulated in WP1193 treatment in hypoxia. On the other hand, fewer proteins in the VEGF, chemokine and apoptosis signaling were affected in hypoxic cells compared to normoxic. In all those cases, the amplitude of the protein changes was greater in normoxic cells compared to hypoxic, which suggests that hypoxic cells have a greater resistance to the therapeutic effects of WP1193.⁴²

Eight proteins known to directly interact with STAT3 were measured in this assay (Table 1). The effect on the STAT3 signaling pathway of WP1193 in hypoxia resulted in upregulation of FOS,⁸³ protein tyrosine kinase 2 (PTK2)⁸⁴ and karyopherin α 4 (KPNA4). The latter increases the translocation of phospho-STAT3 to the cell nucleus.⁸⁵

Among the most increased proteins in WP1193 treatment of GSC11 cells were brain ankyrin (ANK2), nuclear factor IA (NFIA) and the transporter ABCF1 (Supplementary Table 4, Supporting Information). ANK2 was upregulated 10-fold, whereas in the normoxic cells treated with WP1193, it was increased 5-fold. NFIA, a transcriptional regulator, was increased 3-fold in hypoxic cells, but not in normoxic cells, following WP1193

treatment. ABCF1 was more highly expressed (5-fold increase) in normoxic cells than hypoxic. Increased expression of ABC transporters is frequently observed in drug treatments and is associated with resistance to many chemotherapeutic agents.⁸⁶

Effect of STAT3 Phosphorylation Inhibition and IL-6 Stimulation in Normoxic GSC11 Cells. The IGF1-mediated signaling pathway was activated by IL-6 stimulation to WP1193-treated normoxic cells as compared to normoxic control cells (Supplementary Table 5, Supporting Information). This pathway was not activated measurably in normoxic cells treated with WP1193 only, and the significance was highly attenuated in hypoxic cells treated with WP1193 and IL-6. IGF-1-induced receptor (IGF-1R) is a transmembrane tyrosine kinase protein which promotes activation of downstream signaling cascades including the Ras/Raf/MEK/ERK signaling complex, resulting in stimulation of numerous biological processes that include cell growth and differentiation. Recently, IGF-1 was demonstrated to modulate proliferation and strongly stimulate migration of glioma cell lines *in vitro*.⁸⁷

Two other pathways that were affected included the 14-3-3 mediated signaling and protein ubiquitination pathways. The 14-3-3 proteins are a family of conserved adaptor and scaffolding proteins expressed in all eukaryotic cells. There are seven known 14-3-3 isoforms, and one function is to bind specific phosphoserine/threonine-containing motifs and act as allosteric regulators of several proteins related to cell cycle control, stress responses and transcriptional regulation. Two isoforms, 14-3-3 β and 14-3-3 τ , are expressed in gliomas and their expression levels are correlated with the degree of tumor malignancy.⁸⁸ More proteins in this pathway were affected by the addition of IL-6 to WP1193-treated normoxic cells, compared to treatment with WP1193 only.

The protein ubiquitination pathway plays a major role in the degradation of short-lived or regulatory proteins involved in a variety of cellular processes, including cell cycle, cell proliferation, apoptosis, and transcriptional regulation. Degradation of proteins via the protein ubiquitination pathway involves conjugation of multiple ubiquitin moieties to the target protein and degradation of the polyubiquitinated protein by the 26S proteasome complex. In normoxic cells treated with WP1193 and IL-6, three of the top ten increased proteins were ubiquitin-related (Supplementary Table 5, Supporting Information). Two of the proteins were ubiquitin ligases (UBR7, 13-fold and USP39, 9-fold) and one was a ubiquitin-specific ligase and member of the ubiquitination pathway (UHRF, 4-fold). Changes in ubiquitination pathways may be related to cancer cell responses to chemotherapeutics^{89,90} and experimental results obtained at M.D. Anderson have indicated that WP1193 can increase the degradation of Jak2 and other proteins (unpublished data).

One further observation of the normoxic cellular response to WP1193, with or without IL-6 stimulation was the increased levels of seven proteins related to nitric oxide synthase 2 (NOS2, inducible NOS) regulation (Table 2). Hypoxic GSC11 cells treated with WP1193 and IL-6 did not share this pattern of response. Although the role of iNOS has not been studied previously in glioma stem cells, it has been implicated in GBM pathophysiology⁹¹ and nitrous oxide production has been shown to have a protective effect on neuroblastoma cells.⁹² In neuroblastoma and embryonic neuronal cells, nitric oxide downregulates the neuronal precursor proliferation by downregulating N-Myc expression.⁹³ Other oncogenic transcription factors, such as FOS and JUN are regulated by NO signaling.⁹³

Table 2. Activators of iNOS Observed in the MS Data Set and Their Quantitative Values for the WP1193 and WP1193 + IL-6 Stimulated GSC11 Cells in Normoxia^a

IPI number	symbol	entrez gene name	WP1193	WP1193 + IL-6
IPI00013808	ACTN4	actinin, alpha 4	-1.3	1.1
IPI00746777	ADH5	(incl alcohol dehydrogenase 5 (class III), chi polypeptide	1	1
IPI00218918	ANXA1	annexin A1	1.1	-2.5
IPI00006608	APP	amyloid beta (A4) precursor protein	-1.1	-1.1
IPI00234446	ATF2	activating transcription factor 2	1.1	1.3
IPI00220993	CNP	2',3'-cyclic nucleotide 3' phosphodiesterase	-1.2	-1.2
IPI00017292	CTNNB1	catenin (cadherin-associated protein), beta 1, 88 kDa	1.2	1.2
IPI00019329	DYNLL1	dynein, light chain, LC8-type 1	-1.2	1
IPI00301936	ELAVL1	ELAV (embryonic lethal, abnormal vision)-like 1	1.9	2.2
IPI00020985	EP300	E1A binding protein p300	1.9	1.8
IPI00429191	ETF1	eukaryotic translation termination factor 1	1.6	1.5
IPI00011593	FOSL2	FOS-like antigen 2	1.9	2.3
IPI00012856	FOXO3	forkhead box O3		
IPI00177716	HMGAI	high mobility group AT-hook 1	-1.3	-1.4
IPI00027230	HSP90B1	heat shock protein 90 kDa beta (Grp94), member 1	2.8	2
IPI00008965	JUN	jun oncogene		
IPI00028382	KALRN	kalirin, RhoGEF kinase		
IPI00221240	LNPEP	leucyl/cysteinyl aminopeptidase	-1.3	-1.4
IPI00161119	NFKBIB	nuclear factor of κ light polypeptide gene enhancer in B-cells inhibitor β		
IPI00449049	PARP1	poly (ADP-ribose) polymerase 1	1.6	1.8
IPI00032140	SERPINH1	serpin peptidase inhibitor, clade H, member 1	1.7	1.9
IPI00003527	SLC9A3R1	solute carrier family 9, member 3 regulator 1	1.1	1.3
IPI00306436	STAT3	signal transducer and activator of transcription 3		
IPI00219489	TLR9	toll-like receptor 9	1.1	1.6
IPI00180675	TUBA1A	tubulin, alpha 1a		
IPI00418471	VIM	vimentin	1.1	-1.4

^a Inducible NOS was not quantitated in the mass spectrometric data set, but up-regulation of iNOS was confirmed by Western blot (Figure 6).

Furthermore, nitric oxide production might down-regulate the expression of adhesion molecules such as VCAM,⁹⁴ modulate the cellular response to cytotoxic drug treatment⁹⁵ and induce apoptosis of glioma cells.⁹⁶ Because our phosphoproteomic assay did not quantify iNOS, we measured changes in the protein level by Western blot (Figure 6). Those results indicate an increase in iNOS by WP1193 treatment. Further study will be required to understand the role of iNOS in glioma stem cell response patterns.

Effect of STAT3 Phosphorylation Inhibition and IL-6 Stimulation in Hypoxic GSC11 Cells. The top networks associated with treatment of GSC11 cells with WP1193 and IL-6 were RNA post-transcriptional modification, DNA replication and cancer (Supplementary Table 6, Supporting Information). In comparison to the changes observed in the corresponding data set obtained in normoxia, the 14–3–3 pathway was more affected by hypoxia. Also, chemokine signaling and glycolysis/gluconeogenesis were comparatively more affected in hypoxic cells. A summary of the effect of the treatment on the IL-6 signaling pathway is shown in Figure 10.

Proteins involved in protein synthetic networks were more affected in the hypoxic cells as compared to normoxic, whereas RNA post-transcriptional modification was more highly affected in the normoxic cells. The top fold-change upregulated protein was NFIA (6-fold). NFIA regulates GFAP expression in astrocytes,⁹⁷ and GFAP was upregulated also (1.5-fold) as a result of this treatment. As mentioned previously, NFIA increased 3-fold in the WP1193 treated cells in hypoxia, but no significant increase of GFAP was observed in those cells. An increase in GFAP expression might signify differentiation of the cells toward the glial lineage, but further investigation is needed.

By comparison analysis of the quantitative data from WP1193 treated hypoxic GSC11 cells with and without the addition of

IL-6, it is possible to discern effects caused by IL-6 (Figure 11). In the absence of IL-6, the cellular response is increased protein synthesis and RNA post-transcriptional modification. Also, larger number of proteins related to cancer (106 vs 33) were affected when IL-6 treatment was added. When the effect of IL-6 is examined in normoxic GSC11 cells treated with WP1193, the pattern of response differs in several ways. One similarity is that RNA post-transcriptional modification is enhanced by IL-6 treatment of WP1193-treated normoxic cells. However, proteins involved in cell cycle control and cell death are more impacted in normoxic cells treated only with WP1193.

Conclusion

Our analytical approach, which included phosphoprotein enrichment, chemical tagging with isobaric tags, phosphopeptide enrichment and LC–MS/MS analysis, yielded a large and complex data set. We used data obtained by mesoscale detection of chemokines, fast Western blots of key proteins and pathway analysis software to extract knowledge from the data. The analytical workflow enabled quantitation of pathway changes in GSC11 cancer stem cells in six different treatments and constitutes, to the best of our knowledge, the largest proteomic data set acquired to date from glioma stem cells. The data revealed expected pathway changes in the IL6/STAT3/HIF1 α loop but also provided knowledge of many other pathways changed in response to treatment. Also, pathway analysis revealed a possible explanation (activation of ubiquitination enzymes) for earlier observations that WP1193 induces protein degradation (unpublished data), and provided a hypothesis for activation of iNOS during WP1193 treatment. The differences observed in GSC11 responses to treatments performed in normoxic and hypoxic treatments demonstrates

Effect of IL-6, WP1193 and hypoxia on IL-6 signaling pathway

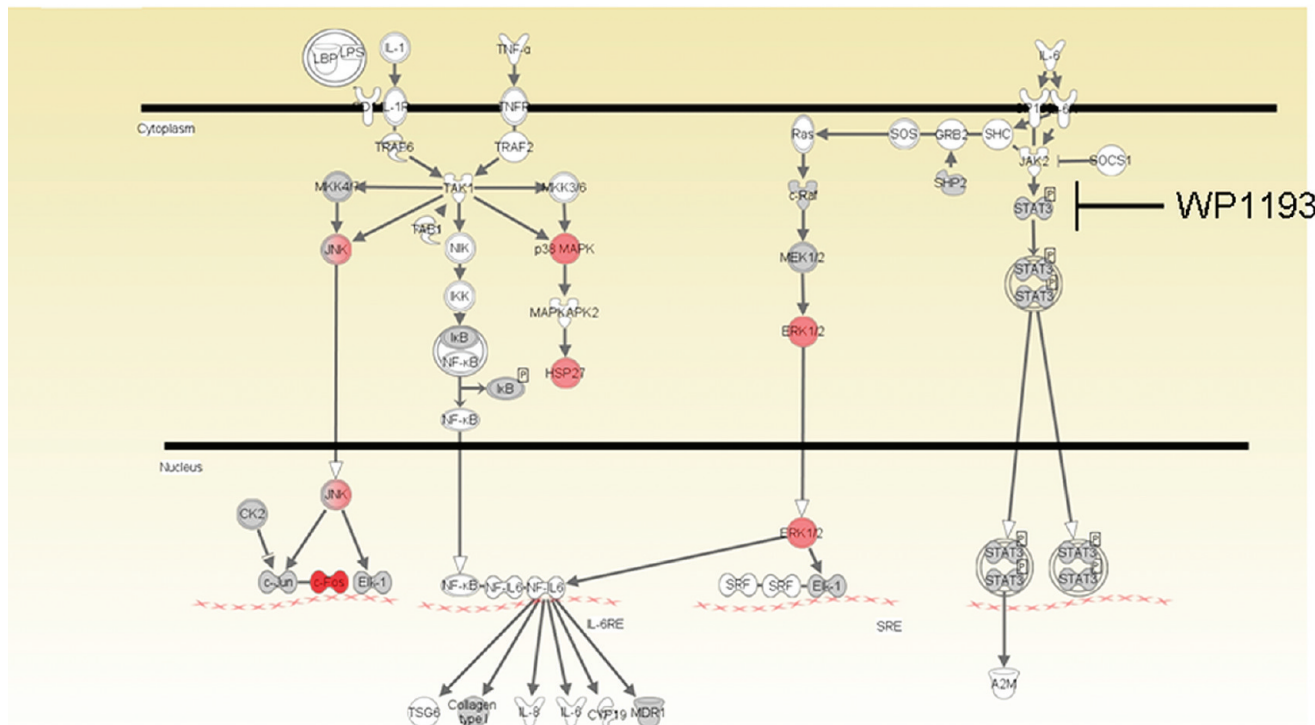


Figure 10. Quantitative protein changes observed in the IL-6 signaling pathway in hypoxic GSC11 cells treated with WP1193 and IL-6, relative to hypoxic control cells. The image was created by overlaying the quantitative proteomic data on the IL-6 signaling pathway in Ingenuity Systems Analysis software. Red indicates increased levels and gray no quantitative change in proteins in cells treated with WP1193 and IL-6 relative to the hypoxic control cells.

Comparison of Effects on Biological Functions in WP1193- and IL-6-treated GSC11 Cells

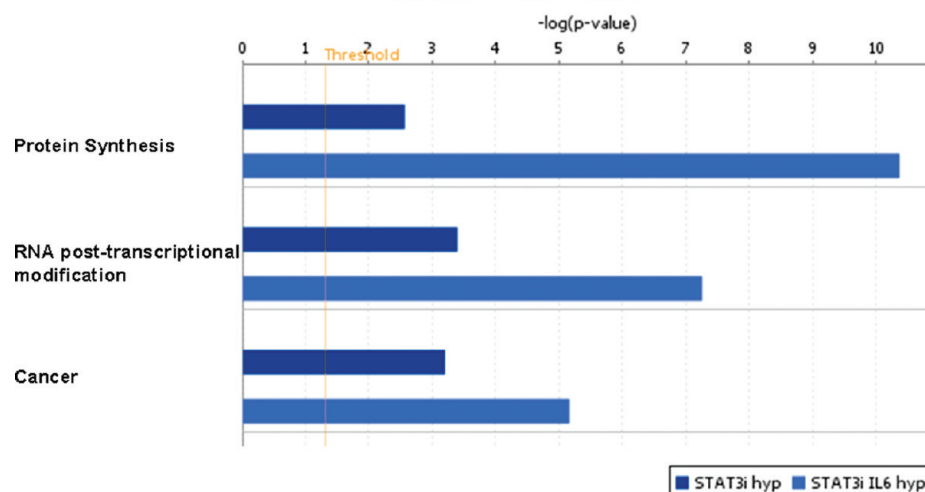


Figure 11. Comparison analysis of biological functions in hypoxic GSC11 cells treated with WP1193 or WP1193 and IL-6. Light blue: WP1193 and IL-6 treatment of hypoxic cells; dark blue: WP1193 treatment of hypoxic cells. Functions identified with a p-value less than 0.05 are determined by Ingenuity analysis based on the number of proteins in the quantitative phosphoproteomic data set compared to the number of proteins that participate in a particular biological function. The addition of IL-6 to WP1193 in GSC11 cells increases the number of proteins associated with protein synthesis, RNA post-transcriptional modification and cancer.

the need to carefully consider oxygen concentrations in *in vitro* experiments that are designed to reflect tumor cell environments. In summary, the application of a quantitative phos-

phoproteomic approach to the analysis of intracellular signaling events in GSC11 glioma stem cells provided deep knowledge about the effects of oxygen concentration, STAT3 phosphory-

lation inhibition and IL-6 stimulation on those *in vitro* cell cultures. Further study of GSC11 and other glioma stem cell lines and biological replicates will be necessary to establish patterns of cellular responses to these treatments. In the future, the combination of studies such as this one with other global analyses such as transcriptomic and glycomic data sets may provide synergistic results that reflect both intracellular and cell surface responses to treatment.

Acknowledgment. We thank Arumugam Jayakumar (MDACC) for providing the MSD data. This work was supported in part by the Dr. Marnie Rose Foundation, the John C. Merchant Foundation, and the CERN Foundation. Dr. Jingjing Ye (Pfizer) and Dr. Darryl Gietzen (Ingenuity Systems) are acknowledged for helpful discussions.

Supporting Information Available: Supplementary Table 1. Comprehensive list of protein and peptide assignments in this study, their molecular weights, post-translational modifications, probability scores, and normalized quantitative reporter ion intensities. Reporter ion 126 is derived from the normoxic GSC11 control, 127 from the hypoxic control, 128 from the WP1193-treated normoxic cells, 129 from the WP1193 hypoxic cells, 130 from normoxic cells treated with WP1193 and IL-6, and 131 from the hypoxic cells treated with WP1193 and IL-6. Supplementary Table 2. Summary report, generated by IPA pathway analysis, of the effect of hypoxia on GSC11 cells. Supplementary Table 3. Summary report, generated by IPA pathway analysis, of the effect of WP1193 on normoxic GSC11 cells. Supplementary Table 4. Summary report, generated by IPA pathway analysis, of the effect of WP1193 and hypoxia on GSC11 cells. Supplementary Table 5. Summary report, generated by IPA pathway analysis, of the effect of WP1193 and IL-6 stimulation on normoxic GSC11 cells. Supplementary Table 6. Summary report, generated by IPA pathway analysis, of the effect of WP1193, IL-6 stimulation and hypoxia on GSC11 cells. This material is available free of charge via the Internet at <http://pubs.acs.org>.

References

- (1) Al-Hajj, M.; Wicha, M. S.; Benito-Hernandez, A.; Morrison, S. J.; Clarke, M. F. Prospective identification of tumorigenic breast cancer cells. *Proc. Natl. Acad. Sci. U.S.A.* **2003**, *100* (7), 3983–3988.
- (2) Bhatia, M.; Wang, J. C.; Kapp, U.; Bonnet, D.; Dick, J. E. Purification of primitive human hematopoietic cells capable of repopulating immune-deficient mice. *Proc. Natl. Acad. Sci. U.S.A.* **1997**, *94* (10), 5320–5325.
- (3) Bonnet, D.; Dick, J. E. Human acute myeloid leukemia is organized as a hierarchy that originates from a primitive hematopoietic cell. *Nat. Med.* **1997**, *3* (7), 730–737.
- (4) Burger, P. E.; Xiong, X.; Coetze, S.; Salm, S. M.; Moscatelli, D.; Goto, K.; Wilson, E. L. Sca-1 expression identifies stem cells in the proximal region of prostatic ducts with high capacity to reconstitute prostatic tissue. *Proc. Natl. Acad. Sci. U.S.A.* **2005**, *102* (20), 7180–7185.
- (5) Collins, A. T.; Berry, P. A.; Hyde, C.; Stower, M. J.; Maitland, N. J. Prospective identification of tumorigenic prostate cancer stem cells. *Cancer Res.* **2005**, *65* (23), 10946–10951.
- (6) Collins, A. T.; Habib, F. K.; Maitland, N. J.; Neal, D. E. Identification and isolation of human prostate epithelial stem cells based on alpha(2)beta(1)-integrin expression. *J. Cell Sci.* **2001**, *114* (Pt 21), 3865–3872.
- (7) Esposito, I.; Kleef, J.; Bischoff, S. C.; Fischer, L.; Collecchi, P.; Iorio, M.; Bevilacqua, G.; Büchler, M. W.; Friess, H. The stem cell factor-c-kit system and mast cells in human pancreatic cancer. *Lab. Invest.* **2002**, *82* (11), 1481–1492.
- (8) Galli, R.; Binda, E.; Orfanelli, U.; Cipelletti, B.; Gritti, A.; De Vitis, S.; Fiocco, R.; Foroni, C.; Dimeco, F.; Vescovi, A. Isolation and characterization of tumorigenic, stem-like neural precursors from human glioblastoma. *Cancer Res.* **2004**, *64*, 7011–7021.
- (9) Gibbs, C. P.; Kukekov, V. G.; Reith, J. D.; Tchigrinova, O.; Suslov, O. N.; Scott, E. W.; Ghivizzani, S. C.; Ignatova, T. N.; Steindler, D. A. Stem-like cells in bone sarcomas: implications for tumorigenesis. *Neoplasia* **2005**, *7* (11), 967–976.
- (10) Hemmati, H. D.; Nakano, I.; Lazareff, J. A.; Masterman-Smith, M.; Geschwind, D. H.; Bronner-Fraser, M.; Kornblum, H. I. Cancerous stem cells can arise from pediatric brain tumors. *Proc. Natl. Acad. Sci. U.S.A.* **2003**, *100* (25), 15178–83.
- (11) Lapidot, T.; Sirard, C.; Vormoor, J.; Murdoch, B.; Hoang, T.; Caceres-Cortes, J.; Minden, M.; Paterson, B.; Caliguri, M. A.; Dick, J. E. A cell initiating human myeloid leukemia after transplantation into SCID mice. *Nature* **1994**, *432* (7015), 396–401.
- (12) Li, C.; Heidt, D. G.; Dalerba, P.; Burant, C. F.; Zhang, L.; Adsay, V.; Wicha, M.; Clarke, M. F.; Simeone, D. M. Identification of pancreatic cancer stem cells. *Cancer Res.* **2007**, *67* (3), 1030–1037.
- (13) O'Brien, C. A.; Pollett, A.; Gallinger, S.; Dick, J. E. A human colon cancer cell capable of initiating tumor growth in immunodeficient mice. *Nature* **2007**, *445* (7123), 106–110.
- (14) Olempska, M.; Eisenach, P. A.; Ammerpohl, O.; Ungefroren, H.; Fandrich, F.; Kalthoff, H. Detection of tumor stem cell markers in pancreatic carcinoma cell lines. *Hepatobiliary Pancreatic Dis. Int.* **2007**, *6* (1), 92–97.
- (15) Patrawala, L.; Calhoun, T.; Schneider-Broussard, R.; Li, H.; Bhatia, B.; Tang, S.; Reilly, J. G.; Chandra, D.; Zhou, J.; Claypool, K.; Coglan, L.; Tang, D. G. Highly purified CD44+ prostate cancer cells from xenograft human tumors are enriched in tumorigenic and metastatic progenitor cells. *Oncogene* **2006**, *25* (12), 1696–708.
- (16) Prince, M. E.; Sivanandan, R.; Kaczorowski, A.; Wolf, G. T.; Kaplan, M. J.; Dalerba, P.; Weissman, I. L.; Clarke, M. F.; Ailles, L. E. Identification of a subpopulation of cells with cancer stem cell properties in head and neck squamous cell carcinoma. *Proc. Natl. Acad. Sci. U.S.A.* **2007**, *104* (3), 973–978.
- (17) Ricci-Vitiani, L.; Lombardi, D. G.; Pilozzi, E.; Biffoni, M.; Todaro, M.; Peschle, C.; DeMaria, R. Identification and expansion of human colon-cancer-initiating cells. *Nature* **2007**, *445* (7123), 111–115.
- (18) Richardson, G. D.; Robson, C. N.; Lang, S. H.; Neal, D. E.; Maitland, N. J.; Collins, A. T. CD133, a novel marker for human prostatic epithelial stem cells. *J. Cell Sci.* **2004**, *117* (Pt 16), 3539–45.
- (19) Singh, S. K.; Clarke, I. D.; Terasaki, M.; Bonn, V. E.; Hawkins, C.; Squire, J.; Dirks, P. Identification of a cancer stem cell in human brain tumors. *Cancer Res.* **2003**, *63* (18), 5821–5828.
- (20) Singh, S. K.; Hawkins, C.; Clarke, I. D. Identification of human brain tumor initiating cells. *Nature* **2004**, *432* (7015), 396–401.
- (21) Taylor, M. D.; Poppleton, H.; Fuller, C.; Su, X.; Liu, Y.; Jensen, P.; Magdaleno, S.; Dalton, J.; Calabrese, C.; Board, J.; Macdonald, T.; Rutka, J.; Guha, A.; Gajjar, A.; Curran, T.; Gilbertson, R. J. Radial glia cells are candidate stem cells of ependymoma. *Cancer Cell* **2005**, *8* (4), 323–335.
- (22) Wente, M. N.; Jain, A.; Kono, E.; Berberat, P. O.; Giese, T.; Reber, H. A.; Friess, H.; Büchler, M. W.; Reiter, R. E.; Hines, O. J. Prostate stem cell antigen is a putative target for immunotherapy in pancreatic cancer. *Pancreas* **2005**, *31* (2), 119–125.
- (23) Xin, L.; Lawson, D. A.; Witte, O. N. The Sca-1 cell surface marker enriches for a prostate-regenerating cell subpopulation that can initiate prostate tumorigenesis. *Proc. Natl. Acad. Sci. U.S.A.* **2005**, *102* (19), 6942–6947.
- (24) Yuan, X.; Curtin, J.; Xiong, Y.; Liu, G.; Wachsmann-Hogiu, S.; Farkas, D. L.; Black, K. L.; Yu, J. S. Isolation of cancer stem cells from adult glioblastoma multiforme. *Oncogene* **2004**, *23* (58), 9392–9400.
- (25) Eyer, C. E.; Rich, J. N. Survival of the fittest: cancer stem cells in therapeutic resistance and angiogenesis. *J. Clin. Oncol.* **2008**, *26* (17), 2839–2845.
- (26) Clarke, M. F.; Dick, J. E.; Dirks, P.; Eaves, C. J.; Jamieson, C. H.; Jones, D. L.; Visvader, J.; Weissman, I. L.; Wahl, G. M. Cancer stem cells—perspectives on current status and future directions: AACR workshop on cancer stem cells. *Cancer Res.* **2006**, *66* (19), 9339–9344.
- (27) Reynolds, B. A.; Tetzlaff, W.; Weiss, S. A multipotent EGF-responsive striatal embryonic progenitor cell produces neurons and astrocytes. *J. Neurosci.* **1992**, *12* (11), 4565–4574.
- (28) Reynolds, B. A.; Weiss, S. Generation of neurons and astrocytes from isolated cells of the adult mammalian central nervous system. *Science* **1992**, *255* (5052), 1707–1710.
- (29) Ignatova, T. N.; Kukekov, V. G.; Laywell, E. D.; Suslov, O. N.; Vrionis, F. D.; Steindler, D. A. Human cortical glial tumors contain neural stem-like cells expressing astroglial and neuronal markers in vitro. *Glia* **2002**, *39* (3), 193–206.
- (30) Jiang, H.; Gomez-Manzano, C.; Aoki, H.; Alonso, M. M.; Kondo, S.; McCormick, F.; Xu, J.; Bekele, B. N.; Colman, H.; Lang, F. F.; Fueyo, J. Examination of the therapeutic potential of delta-24-RGD

- in brain tumor cells: Role of autophagic cell death. *J. Natl. Cancer Inst.* **2007**, *99*, 1410–1414.
- (31) Sai, K.; Shuzhen, W.; Balasubramanian, V.; Aldape, K.; Lang, F. F.; Conrad, C. A.; Madden, T.; Yung, W. K. A.; Priebe, W.; Colman, H. A novel small-molecule inhibitor of the JAK2/STAT3 pathway blocks self-renewal and induces apoptosis in brain tumor stem cells. In *13th Annual Meeting of the Society for Neuro-oncology*; Las Vegas, NV, 2008; Duke University Press.
 - (32) Lang, S. A.; Moser, C.; Gaumann, A.; Klein, D.; Glockzin, G.; Popp, F. C.; Dahlke, M. H.; Piso, P.; Schlitt, H. J.; Geissler, E. K.; Stoeltzing, O. Targeting heat shock protein 90 in pancreatic cancer impairs insulin-like growth factor-I receptor signaling, disrupts an interleukin-6/signal-transducer and activator of transcription 3/hypoxia-inducible factor-1alpha autocrine loop, and reduces orthotopic tumor growth. *Clin. Cancer Res.* **2007**, *13* (21), 6459–6468.
 - (33) Heikkila, K.; Ebrahim, S.; Lawlor, D. A. Systematic review of the association between circulations interleukin-6 (IL-6) and cancer. *Eur. J. Cancer* **2008**, *44*, 937–945.
 - (34) Jung, J. E.; Lee, H. G.; Cho, I. H.; Chung, D. H.; Yoon, S.-H.; Yang, Y. M.; Lee, J. W.; Choi, S.; Park, J.-W.; Ye, S.-K.; Chung, M. H. STAT3 is a potential modulator of HIF-1-mediated VEGF expression in human renal carcinoma cells. *Faseb J.* **2005**, *19*, 1296–1298.
 - (35) Haura, E. B.; Turkson, J.; Jove, R. Mechanisms of disease:insights into the emerging role of signal transducers and activators of transcription in cancer. *Nat. Clin. Pract.* **2005**, *2* (6), 315–323.
 - (36) Yu, H.; Kortylewski, M.; Pardoll, D. Crosstalk between cancer and immune cells:role of STAT3 in the tumour microenvironment. *Nat. Rev. Immunol.* **2007**, *7*, 41–51.
 - (37) Heimberger, A. B.; Priebe, W. Small molecule inhibitors of p-STAT3: novel agents for treatment of primary and metastatic CNS cancers. *Recent Pat. CNS Drug Discov.* **2008**, *3* (3), 179–188.
 - (38) Lin, L.; Amin, R.; Gallianico, G. I.; Glasgow, E.; Jogunoori, W.; Jessup, J. M.; Zasloff, M.; Marshall, J. L.; Shetty, K.; Johnson, L.; Mishra, L.; He, A. R. The STAT3 inhibitor NSC 74859 is effective in hepatocellular cancers with disrupted TGF-beta signaling. *Oncogene* **2009**, *28*, 961–972.
 - (39) Schafer, Z. T.; Brugge, J. S. IL-6 involvement in epithelial cancers. *J. Clin. Invest.* **2007**, *117* (12), 3660–3663.
 - (40) Grivennikov, S.; Karin, E.; Terzic, E.; Mucida, D.; Yu, G.-Y.; Vallabhapurapu, S.; Scheller, J.; Rose-John, S.; Cheroutre, H.; Eckmann, L.; Karin, M. IL-6 and Stat3 are required for survival of intestinal epithelial cells and development of colitis-associated cancer. *Cancer Cell* **2009**, *15*, 103–113.
 - (41) McCord, A. M.; Jamal, M.; Shankavarum, U. T.; Lang, F. F.; Camphausen, K.; Tofilon, P. J. Physiologic oxygen concentration enhances the stem-like properties of CD133+ human glioblastoma cells in vitro. *Mol. Cancer Res.* **2009**, *7* (4), 489–497.
 - (42) Li, Z.; Bao, S.; Wu, Q.; Wang, H.; Eyler, C.; Sathornsumetee, S.; Shi, Q.; Cao, Y.; Lathia, J.; McLendon, R. E.; Hjelmeland, A. B.; Rich, J. N. Hypoxia-inducible factors regulate tumorigenic capacity of glioma stem cells. *Cancer Cell* **2009**, *15*, 501–513.
 - (43) Viemann, D.; Schmidt, M.; Tenbrock, K.; Schmid, S.; Muller, V.; Klimmek, K.; Ludwig, S.; Roth, J.; Goebeler, M. The contact allergen nickel triggers a unique inflammatory and proangiogenic gene expression pattern via activation of NF-kappaB and hypoxia-inducible factor-1alpha. *J. Immunol.* **2007**, *178* (5), 3198–3207.
 - (44) Boehm, A. M.; Putz, S.; Altenhofer, D.; Sickmann, A.; Falk, M. Precise protein quantification based on peptide quantification using iTRAQ. *BMC Bioinformatics* **2007**, *8*, 214.
 - (45) de la Fuente van Bentem, S.; Mentzen, W. I.; de la Fuente, A.; Hirt, H. Towards functional phosphoproteomics by mapping differential phosphorylation events in signaling networks. *Proteomics* **2008**, *8*, 4453–4465.
 - (46) Macek, B.; Mann, M.; Olsen, J. V. Global and site-specific quantitative phosphoproteomics:Principles and applications. *Annu. Rev. Pharmacol.* **2009**, *49*, 199–221.
 - (47) Nita-Lazar, A.; Saito-Benz, H.; White, F. M. Quantitative phosphoproteomics by mass spectrometry:Past, present and future. *J. Proteome Res.* **2008**, *8*, 4433–4443.
 - (48) Swaney, D. L.; Wenger, C. D.; Thomson, J. A.; Coon, J. J. Human embryonic stem cell phosphoproteome revealed by electron transfer dissociation tandem mass spectrometry. *Proc. Natl. Acad. Sci. U.S.A.* **2009**, *106* (4), 995–1000.
 - (49) Thingholm, T. E.; Larsen, M. R.; Ingrell, C. R.; Kassem, M.; Jensen, O. N. TiO-based phosphoproteomic analysis of the plasma membrane and the effects of phosphatase inhibitor treatment. *J. Proteome Res.* **2008**, *7* (8), 3304–3313.
 - (50) Beausoleil, S. A.; Jedrychowski, M.; Schwartz, D.; Elias, J. E.; Villen, J.; Li, J.; Cohn, M. A.; Cantley, L. C.; Gygi, S. Large-scale characterization of HeLa cell nuclear phosphoproteins. *Proc. Natl. Acad. Sci. U.S.A.* **2004**, *101* (33), 12130–12135.
 - (51) Huang, P. H.; Mukasa, A.; Bonavia, R.; Flynn, R. A.; Brewer, Z. E.; Cavenee, W. K.; Furnari, F. B.; White, F. M. Quantitative analysis of EGFRvIII cellular signaling networks reveals a combinatorial therapeutic strategy for glioblastoma. *Proc. Natl. Acad. Sci. U.S.A.* **2007**, *104* (31), 12867–12872.
 - (52) Kruger, M.; Kratchmarova, I.; Blagoev, B.; Tseng, Y.-H.; Kahn, C. R.; Mann, M. Dissection of the insulin pathway via quantitative phosphoproteomics. *Proc. Natl. Acad. Sci. U.S.A.* **2008**, *105* (7), 2451–2456.
 - (53) Wilson-Grady, J. T.; Villen, J.; Gygi, S. Phosphoproteome analysis of fission yeast. *J. Proteome Res.* **2008**, *7* (3), 1088–1097.
 - (54) Abu-Farha, M.; Elisma, F.; Zhou, H.; Tian, R.; Zhou, H.; Asmer, M. S.; Figgeys, D. Proteomics: From technology developments to biological applications. *Anal. Chem.* **2009**, *81*, 4686–4699.
 - (55) Dayon, L.; Hainard, A.; Licker, V.; Turck, N.; Kuhn, K.; Hochstrasser, D. F.; Burkhardt, P. R.; Sanchez, J.-C. Relative quantification of proteins in human cerebrospinal fluids by MS/MS using 6-plex isobaric tags. *Anal. Chem.* **2008**, *80* (8), 2921–2931.
 - (56) van Ulsen, P.; Kuhn, K.; Prinz, T.; Legner, H.; Schmid, P.; Baumann, C.; Tommassen, J. Identification of proteins of *Neisseria meningitidis* induced under iron-limiting conditions using the isobaric tandem mass tag (TMT) labeling approach. *Proteomics* **2009**, *9* (7), 1771–1781.
 - (57) Albuquerque, C. P.; Smolka, M. B.; Payne, S. H.; Bafna, V.; Eng, J.; Zhou, H. A multidimensional chromatography technology for in-depth phosphoproteome analysis. *Mol. Cell. Proteomics* **2008**, *7*, 1389–1396.
 - (58) McNulty, D. E.; Annan, R. S. Hydrophilic interaction chromatography reduces the complexity of the phosphoproteome and improves global phosphopeptide isolation and detection. *Mol. Cell. Proteomics* **2008**, *7*, 971–980.
 - (59) McNulty, D. E.; Annan, R. S. Hydrophilic interaction chromatography for fractionation and enrichment of the phosphoproteome. *Methods Mol. Biol.* **2009**, *527*, 93–105.
 - (60) Bradford, M. M. A rapid and sensitive method for the quantitation of microgram quantities of protein utilizing the principle of protein-dye binding. *Anal. Biochem.* **1976**, *72*, 248–254.
 - (61) Kocher, T.; Pichler, P.; Schutzbier, M.; Stingl, C.; Kaul, A.; Teucher, N.; Hasenfuss, G.; Pennington, J. M.; Mechteder, K. High precision quantitative proteomics using iTRAQ on an LTQ orbitrap: a new mass spectrometric method combining the benefits of all. *J. Proteome Res.* **2009**, *8*, 4743–4752.
 - (62) Olsen, J. V.; Macek, B.; Lange, O.; Makarov, A.; Horning, S.; Mann, M. Higher-energy C-trap dissociation for peptide modification analysis. *Nat. Methods* **2007**, *4* (9), 709–712.
 - (63) Glantz, S. A. *Primer of Biostatistics*, 6th ed.; McGraw-Hill Medical Publishing: New York, 2005.
 - (64) Brat, D. J.; Bellail, A. C.; Van Meir, E. G. The role of interleukin-8 and its receptors in gliomagenesis and tumoral angiogenesis. *Neuro Oncol.* **2005**, *7* (2), 122–133.
 - (65) Peng, X. H.; Karna, P.; Cao, Z.; Jiang, B. H.; Zhou, M.; Yang, L. Cross-talk between epidermal growth factor receptor and hypoxia-inducible factor-1-alpha signal pathways increases resistance to apoptosis by up-regulating survivin gene expression. *J. Biol. Chem.* **2006**, *281* (36), 25903–25914.
 - (66) Heddleston, J. M.; Li, Z.; McLendon, R. E.; Hjelmeland, A. B.; Rich, J. N. The hypoxic environment maintains glioblastoma stem cells and promotes reprogramming towards a cancer stem cell phenotype. *Cell Cycle* **2009**, *8* (20), 1–11.
 - (67) Ow, S. Y.; Salim, M.; Noirel, J.; Evans, C.; Rehman, I.; Wright, P. C. iTRAQ underestimation in simple and complex mixtures: The good, the bad and the ugly. *J. Proteome Res.* **2009**, *8*, 5347–5355.
 - (68) Bertout, J. A.; Patel, S. A.; Simon, M. The impact of O2 availability on human cancer. *Nat. Rev. Cancer* **2008**, *8* (12), 967–975.
 - (69) Takeda, K.; Cowan, A.; Fong, G. H. Essential role for prolyl hydroxylase domain protein 2 in oxygen homeostasis of the adult vascular system. *Circulation* **2007**, *116* (7), 774–781.
 - (70) Appelhoff, R. J.; Tian, Y. M.; Raval, R. R.; Turley, H.; Harris, A. L.; Pugh, C. W.; Ratcliffe, P. J.; Gleadle, J. M. Differential function of the prolyl hydroxylases PHD1, PHD2, PHD3 in the regulation of hypoxia-inducible factor. *J. Biol. Chem.* **2004**, *279* (37), 38458–38465.
 - (71) Gaiddon, C.; Moorthy, N. C.; Prives, C. Interaction of human APEX1 protein and human TP53 protein increases activation of human TP53 protein. *EMBO J.* **1999**, *18* (20), 5609–5621.
 - (72) Robertson, K. A.; Bullock, H. A.; Xu, Y.; Tritt, R.; Zimmerman, E.; Ulbright, T. M.; Foster, R. S.; Einhorn, L. H.; Kelley, M. R. Altered expression of Ape1/ref-1 in germ cell tumors and overexpression in NT2 cells confers resistance to bleomycin and radiation. *Cancer Res.* **2001**, *61* (5), 2220–5.

- (73) Flügel, D.; Görlich, A.; Michiels, C.; Kietzmann, T. Glycogen synthase kinase 3 phosphorylates Hypoxia-Inducible Factor 1 α and mediates its destabilization in a VHL-independent manner. *Mol. Cell. Biol.* **2007**, *27* (9), 3253–65.
- (74) Chakravarti, A.; Delaney, M. A.; Noll, E.; Black, P. M.; Loeffler, J. S.; Muzikansky, A.; Dyson, N. J. Prognostic and pathologic significance of quantitative protein expression profiling in human gliomas. *Clin. Cancer Res.* **2001**, *7* (8), 2387–95.
- (75) Mehran-Shai, R.; Chen, C. D.; Shi, T.; Horvath, S.; Nelson, S. F.; Reichardt, J. K.; Sawyers, C. L. Insulin growth factor-binding protein 2 is a candidate biomarker for PTEN status and PI3K/Akt pathway activation in glioblastoma and prostate cancer. *Proc. Natl. Acad. Sci. U.S.A.* **2007**, *104* (13), 5563–8.
- (76) Bindu, A. V.; Kabbani, N.; Lin, R.; Levenson, R. D2 and D3 dopamine receptor cell surface localization mediated by interaction with protein 4.1N. *Mol. Pharmacol.* **2002**, *62* (3), 507–13.
- (77) Coleman, S. K.; Cai, C.; Mottershead, D. G.; Haapalahti, J. P.; Keinanen, K. Surface expression of GluR-D AMPA receptor is dependent on an interaction between its C-Terminal Domain and a 4.1 Protein. *J. Neurosci.* **2003**, *23* (3), 798–806.
- (78) Ye, K.; Compton, D. A.; Lai, M. M.; Walensky, L. D.; Snyder, S. H. Protein 4.1N binding to nuclear mitotic apparatus protein in PC12 cells mediates the antiproliferative actions of nerve growth factor. *J. Neurosci.* **1999**, *19* (24), 10747–10756.
- (79) Pullmann, R.; Juhaszova, M.; de Silanes, I. L.; Kawai, T.; Mazan-Mamczarz, K.; Halushka, M. K.; Gorospe, M. Enhanced proliferation of cultured human vascular smooth muscle cells linked to increased function of RNA-binding protein HuR. *J. Biol. Chem.* **2005**, *280* (24), 22819–22826.
- (80) He, H.; Nilsson, C. L.; Emmett, M. R.; Marshall, A. G.; Kroes, R. A.; Moskal, J. R.; Ji, Y.; Colman, H.; Lang, F. F.; Conrad, C. A. Glycomic and transcriptomic response of GSC11 glioblastoma stem cells to STAT3 inhibition and serum-induced differentiation. Submitted.
- (81) Kizhatil, K.; Davis, J. Q.; Davis, L.; Hoffman, J.; Hogan, B. L.; Bennett, V. Ankyrin-G is a molecular partner of E-cadherin in epithelial cells and early embryos. *J. Biol. Chem.* **2007**, *282* (36), 26552–26561.
- (82) Ross, D. T.; Scherf, U.; Eisen, M. B.; Perou, C. M.; Rees, C.; Spellman, P.; Iyer, V.; Jeffrey, S. S.; Van de Rijn, M.; Waltham, M.; Pergamenschikov, A.; Lee, J. C.; Lashkari, D.; Shalon, D.; Myers, T. G.; Weinstein, J. N.; Botstein, D.; Brown, P. O. Systematic variation in gene expression patterns in human cancer *dlx* lines. *Nat. Genet.* **2000**, *24* (3), 227–235.
- (83) Joo, A.; Aburatani, H.; Morii, E.; Iba, H.; Yoshimura, A. STAT3 and MITF cooperatively induce cellular transformation through up-regulation of c-fos expression. *Oncogene* **2004**, *23* (3), 726–734.
- (84) Xie, B.; Zhao, J.; Kitagawa, M.; Durbin, J.; Madri, J. A.; Guan, J. L.; Fu, X. Y. Focal adhesion kinase activates Stat1 in integrin-mediated cell migration and adhesion. *J. Biol. Chem.* **2001**, *276* (22), 19512–19523.
- (85) Liu, L.; McBride, K. M.; Reich, N. C. STAT3 nuclear import is independent of tyrosine phosphorylation and mediated by importin-alpha3. *Proc. Natl. Acad. Sci. U.S.A.* **2005**, *102* (23), 8150–8155.
- (86) Martin, V.; Xu, J.; Pabbisetty, S. K.; Alonso, M. M.; Liu, D.; Lee, O.-H.; Gumin, J.; Bhat, K. P.; Colman, H.; Lang, F. F.; Fueyo, J.; Gomez-Manzano, C. Tie2-mediated multidrug resistance in malignant gliomas is associated with upregulation of ABC transporters. *Oncogene* **2009**, *28*, 2358–2363.
- (87) Schlenska-Lange, A.; Knupfer, H.; Lange, T. J.; Kiess, W.; Knupfer, M. Cell proliferation and migration in glioblastoma multiforme cell lines are influenced by insulin-like growth factor I in vitro. *Anticancer Res.* **2008**, *28* (2A), 1055–1060.
- (88) Yang, X.; Cao, W.; Lin, H.; Zhang, W.; Lin, W.; Cao, L.; Zhen, H.; Huo, J.; Zhang, X. Isoform-specific expression of 14–3–3 proteins in human astrocytoma. *J. Neurol. Sci.* **2009**, *276* (1–2), 54–59.
- (89) VLachostergios, P. J.; Patrikidou, A.; Daliani, D. D.; Papandreou, C. N. The Ubiquitin-Proteasome System in cancer, a major player in DNA Repair. Part 1: Post-translational regulation. *J. Cell. Mol. Med.* **2009**, published on line June 11, 2009.
- (90) VLachostergios, P. J.; Patrikidou, A.; Daliani, D. D.; Papandreou, C. N. The Ubiquitin-Proteasome System in cancer, a major player in DNA Repair. Part 2: Transcriptional regulation. *J. Cell. Mol. Med.* **2009**, published on line June 11, 2009.
- (91) Lam-Himlin, D.; Espey, M. G.; Perry, G.; Smith, M. A.; Castellani, R. J. Malignant glioma progression and nitric oxide. *Neurochem. Int.* **2006**, *49* (8), 764–768.
- (92) Ciani, E.; Guidi, S.; Della Valle, G.; Perini, G.; Bartesaghi, R.; Contestabile, A. Nitric Oxide Protects Neuroblastoma Cells from Apoptosis Induced by Serum Deprivation through cAMP-response Element-binding Protein (CREB) Activation. *J. Biol. Chem.* **2002**, *277* (51), 49896–902.
- (93) Contestabile, A. Regulation of transcription factors by nitric oxide in neurons and in neural-derived tumor cells. *Prog. Neurobiol.* **2008**, *84* (4), 317–328.
- (94) Khan, B. V.; Harrison, D. G.; Olbrych, R. W.; Medford, R. M. Nitric oxide regulates vascular cell adhesion molecule 1 gene expression and redox-sensitive transcriptional events in human vascular endothelial cells. *Proc. Natl. Acad. Sci. U.S.A.* **1996**, *93*, 9114–9119.
- (95) Yang, D. I.; Yin, J. H.; Mishra, S.; Mishra, R.; Hsu, C. Y. NO-mediated chemoresistance in C6 glioma cells. *Ann. N.Y. Acad. Sci.* **2002**, *962*, 8–17.
- (96) Shinoda, J.; Whittle, I. R. Nitric oxide and glioma: a target for novel therapy. *Br. J. Neurosurg.* **2001**, *15*, 213–220.
- (97) Gopalan, S. M.; Wilczynska, K. M.; Konik, B. S.; Bryan, L.; Kordula, T. Nuclear factor-1-X regulates astrocyte-specific expression of the alpha β -antichymotrypsin and glial fibrillary acidic protein genes. *J. Biol. Chem.* **2006**, *281* (19), 13126–13133.
- (98) Xu, Q.; Briggs, J.; Park, S.; Niu, G.; Kortylewski, M.; Zhang, S.; Gritsko, T.; Turkson, J.; Kay, H.; Semenza, G. L.; Cheng, J. Q.; Jove, R.; Yu, H. Targeting Stat3 blocks both HIF-1 and VEGF expression induced by multiple oncogenic growth signaling pathways. *Oncogene* **2005**, *24* (36), 5552–5560.

PR9007927